



Adsorption of the reactive gray BF-2R dye on orange peel: kinetics and equilibrium studies

Graziele Elisandra do Nascimento, Marta Maria Menezes Bezerra Duarte*, Natália Ferreira Campos, Celmy Maria Bezerra de Menezes Barbosa, Valdinete Lins da Silva

Chemical Engineering Department, Federal University of Pernambuco, Avenida Artur de Sá, s/n, Recife 50740-521, Brazil

Tel. +558121267291; Fax: +558121267278; email: mmmdbuarte@gmail.com

Received 31 January 2013; Accepted 14 March 2013

ABSTRACT

Adsorption of the reactive gray BF-2R dye from an aqueous solution using orange peel as the adsorbent was investigated by the batch method. Experiments characterizing the chemical and physical properties of the adsorbent found that orange peel is a microporous material with a pH_{zpc} 3.9 and containing carboxylic and sulfonic groups. The greatest adsorption capacity was obtained using a 2^3 factorial design for 0.25 g of adsorbent, particle size < 0.419 mm and at 300 rpm. The pseudo-second-order model provided the best fit of the experimental data. The Weber–Morris model indicated that two or more mechanisms control the process. Statistical analysis of the equilibrium studies indicated that there was not a significant difference between the Langmuir and the Fritz–Schlunder models according to an *F*-test. The results showed that orange peel can remove the reactive gray BF-2R dye.

Keywords: Adsorption; Agroindustrial residue; Dye

1. Introduction

The insufficient treatment and improper disposal of industrial effluents constitute serious factors contributing to the deterioration of aquatic ecosystems. Discharging industrial effluents that contain hazardous contaminants, such as phenolics, toxic metals, and dyes, even at low concentrations, negatively impact the environment [1].

Textile, pulp, and paper industries, among others, generate effluents containing coloring agents [2]. The coloring agents, even in small amounts, affect bodies of water not only esthetically but also by reducing the penetration of light through the water surface and

consequently inhibiting photosynthesis, which may cause severe problems such as increased the chemical oxygen demand [1–5].

After undergoing oxidation and reduction in water, these dyes create toxic and hazardous intermediates or substances that further increase the need for their removal from wastewater [6,7].

One of the most important classes of dyes is reactive dye, and their most common reactive groups are the heterocyclic ring-type and vinyl sulfone [8].

Azo reactive dyes are among the largest and most versatile classes of synthetic dyes with the greatest variety of colors. These dyes are characterized by the existence of nitrogen–nitrogen double bonds, and the presence of bright color is due to these azo bonds and

*Corresponding author.

associated chromospheres [9]. One side effect of extensive use of these chemicals is the production of potentially carcinogenic compounds [10,11].

The azo bond is fragile to reductive cleavage, and its degradation products include aromatic amines. The enzymatic breakdown reaction in mammals, including man, is carried out by a class of enzyme named azoreductases, which have different activities and are present in various organs such as liver, kidney, lung, heart, brain, spleen, and muscle tissues. After cleavage of the azo linkage, the component aromatic amines are absorbed in the intestine and excreted in the urine. Aromatic amines comprise a group of chemicals that is associated with severe acute and chronic effects. It has been reported as toxic, mutagenic, and carcinogenic in many types of studies on many species [12].

The reactive gray BF-2R dye was provided by Texpal Industry located in Valinhos-SP. According to the dye data sheet provided by the manufacturer, the dye is an azo dye bifunctional colorant comprised of chromophores linked to two reactive groups: a vinyl sulfone and a chlorotriazine group. This dye has a very intense gray color, and it is used as a base to obtain intense dark colors, such as deep black.

Thus, color removal from wastewater is a major concern for environmentalists and researchers [3,13]. Methods such as coagulation [14], flocculation [15], froth flotation [16], filtration [17], ion exchange [18], aerobic and anaerobic treatment [19–21], and reverse osmosis [22] are commonly used to treat effluents, but these methods are not completely effective or economically advantageous in treating these compounds due to cost factors and the formation of by-products [3,23].

Among the various methodologies used in wastewater treatment, adsorption has attracted interest, because it is efficient, easy to operate, insensitive to toxic substances, and less operationally expensive. Recovering the adsorbed material and regenerating the adsorbent is possible in adsorption processes [3,24–31].

The most widely used adsorbent is activated carbon, because it is efficient. The preparation of this material, however, involves expensive chemicals and a great amount of energy consumption, resulting in a high cost [32].

Thus, researchers have been searching for alternative adsorbents such as agro-industrial residues, because these are abundant, biodegradable, inexpensive and efficient in dye adsorption [33]. Some studies have been conducted using the banana peels [34], orange peels [35], de-oiled soya [36–39], green coconut mesocarp [40,41], wood apple shell [42], grapefruit peels [1], hen feathers [25,26], ginger waste [4], passion fruit [43], and green coconut fibers [44].

Amino, carboxyl, thiol, and phosphate functional groups present on the cell wall of the biosorbent are responsible for the removal of dyes from the textile effluents. Biosorption of the dyes on the cell surface appears to be a quick process and is often completed in a matter of hours [29].

Given the above, this study aimed to evaluate the adsorption process using orange peel, agro residue as adsorbents in the removal of reactive gray BF-2R dye.

2. Experimental

2.1. Dye solution

The concentration of the reactive gray BF-2R dye was measured before and after contact with the adsorbent using UV-vis spectrometry at a wavelength of greater absorbance (596 nm). The analytical parameters were linear range of $5\text{--}120\text{ mg L}^{-1}$, with a regression coefficient (R^2) of 0.994, a detection limit of 0.1 mg L^{-1} and a quantitation limit of 0.3 mg L^{-1} . Assays were performed in a finite bath system. Blank assays were also developed using the same procedure.

2.2. Preparation of adsorbent material

The orange peels were washed with water, dried at 60°C , ground in a knife mill (Tecnal) and thoroughly washed again with distilled water. After washing, samples were dried again at 60°C and then stored in a series of Tyler sieves of particle sizes $<0.419\text{ mm}$, $0.419\text{--}0.592\text{ mm}$, and $0.592\text{--}0.837\text{ mm}$.

2.3. Characterization of the adsorbent material

2.3.1. Measurement of surface area by the adsorption/desorption of N_2 (BET)

The adsorbent was characterized by adsorption/desorption of nitrogen using the BET method to determine the specific surface area and pore volume of the adsorbent materials. The surface area of the material was determined by N_2 adsorption at $77 \pm 5\text{ K}$ using Quantachrome Surface Area and Pore Size Analyzer Nova 1000e. Prior to analysis, 0.15 g of the sample was pretreated at 60°C under vacuum (DEGASS) for 3 h. This treatment was aimed to remove moisture from the surface of the solid.

2.3.2. pH_{zpc} of the adsorbent

The pH at the point of zero charge (pH_{zpc}) of the adsorbent was estimated by pH measurements before

and after contact with the solid, following the methodology of Schimmel [45]. In assays, 0.25 g of the adsorbent was placed in 50 mL of a solution with pH ranging from 2 to 10. The solution pH was adjusted with HCl (0.1 mol L^{-1}) or NaOH (0.1 mol L^{-1}) solutions. The solutions were agitated for 24 h and then filtered, and the pH was measured. The graph of the variation of pH ($\text{pH}_{\text{final}} - \text{pH}_{\text{initial}}$) vs. $\text{pH}_{\text{initial}}$ was constructed, and the pH_{zpc} value was estimated from this graph.

2.3.3. Fourier transform infrared spectroscopy

Functional groups on the surface of the orange peel were identified using infrared spectroscopy. The absorption spectra were obtained in an infrared spectrometer (FT-IR IRAffinity Shimadzu) using a diffuse reflectance accessory (Pike Technologies Inc., Model: EasiDiff TM). The spectra were recorded in the region of $4,000\text{--}500 \text{ cm}^{-1}$.

2.4. Adsorption experiments

The amount of dye adsorbed per gram of adsorbent was calculated using Eq. (1).

$$q = \frac{(C_0 - C_f)V}{M} \quad (1)$$

where q is the adsorption capacity (mg g^{-1}), C_0 and C_f are the initial and final concentrations, respectively, of dye in solution (mg L^{-1}), V is the volume of solution used (L), and M is the adsorbent mass (g).

2.4.1. Effect of dye solution pH

The effect of dye solution pH was investigated by performing the adsorption experiments with the dye solution at various pH values from 2–10. The pH of each solution was adjusted to the desired value with either diluted HCl (0.1 mol L^{-1}) or NaOH (0.1 mol L^{-1}) solutions. Orange peel (0.1 g) was blended in 50 mL of dye solution (100 mg L^{-1}) and was agitated at 300 rpm for 120 min.

2.4.2. Adsorbent concentration study

Assays were performed to assess the concentration of adsorbent to compare the dye removal percentage and the adsorption capacity of the orange peel.

The effect of concentration of the adsorbent in the adsorption of reactive gray BF-2R dye was analyzed using 0.25, 0.50, 0.75, 1.00, 1.25, 1.50, and 2.00 g masses

of orange peel. The tests were conducted in Erlenmeyer flasks containing 50 mL of the dye solution at a concentration of 100 mg L^{-1} , a pH that had been defined in the previous section, and this solution was agitated at 300 rpm for 120 min.

2.4.3. Factorial design

A factorial design was conducted to evaluate the influence of the adsorbent mass variables – M (0.25, 0.50 and 0.75 g), the adsorbent particle size – PS ($<0.419 \text{ mm}$, $0.419\text{--}0.592 \text{ mm}$ and $0.592\text{--}0.837 \text{ mm}$) and stirring speed – SS (0, 150 and 300 rpm), on the adsorptive process. The assays were performed in random order. The factorial design was type 2^3 with a triplicate central point to ensure reproducibility of the experimental data and resulted in 11 experiments. The adsorptive capacity, q (mg g^{-1}) was used to assess the efficiency of the process.

Erlenmeyer flasks were used for these experiments, each containing 50 mL of the dye at a concentration of 100 mg L^{-1} using HCl (0.1 mol L^{-1}) to adjust the pH. Assays were performed at laboratory temperature ($25 \pm 2^\circ\text{C}$) with the aid of a shaker table. The calculations of the effects of the factors, including interactions with their respective standard errors, obtained an empirical model able to predict the adsorption capacity in the range of study for the three variables. These calculations were performed according to Barros Neto et al. [46], using the program Statistica 6.0.

2.4.4. Kinetics and equilibrium adsorption study

Using the conditions established by the factorial design 2^3 , we carried out the kinetics study. Independent experiments were performed at 0, 5, 7, 10, 15, 30, 45, 60, 90, 120, 180, 240, 300, and 360 min for concentrations of 20, 35, 55, 65, 100, and 120 mg L^{-1} .

The experimental data obtained from the equilibrium and kinetics studies were adjusted by mathematical models using a nonlinear regression method (Origin 8.0). The model parameters were obtained by minimizing the sum of squared deviations between the experimental and predicted values. The model fit was assessed by the relative standard deviations (σ_i) and R^2 . The performances of the better fitting models were compared using an F -test [47]. F_{cal} is defined using Eq. (2).

$$F_{\text{cal}} = \frac{S_R^2(A)}{S_R^2(B)} \quad (2)$$

where $S_R^2(A)$ and $S_R^2(B)$ represent the models variances of models *A* and *B*, respectively, $S_R(A) > S_R(B)$. If $F_{cal} > F_{tab}$, then model *B* provides a better fit than model *A* at a 95% level of confidence.

Pseudo-first-order and pseudo-second-order kinetic models were used. Additionally, the Weber–Morris intraparticle diffusion model was used to evaluate the adsorption mechanism. The adsorption kinetics is usually described by pseudo-first-order (Eq. (3)) and pseudo-second-order (Eq. (4)) models [48].

$$\frac{dq_t}{dt} = k_1(q_e - q_t) \quad (3)$$

$$\frac{dq_t}{dt} = k_2(q_e - q_t)^2 \quad (4)$$

where q_e and q_t are the quantities of dye adsorbed (mg g^{-1}) at equilibrium and time t , respectively, k_1 is the adsorption constant of the pseudo-first-order equation (min^{-1}), and k_2 is the adsorption constant of the pseudo-second-order equation ($\text{g mg}^{-1} \text{min}^{-1}$).

According to Weber and Morris, the intraparticle diffusion is the rate-determining step because the removal of the adsorbate varies with the square root of time [49]. Thus, k_{dif} , the intraparticle diffusion coefficient, can be defined by Eq. (5).

$$q_t = k_{dif}t^{1/2} + C \quad (5)$$

where C (mg g^{-1}) is a constant related to diffusion resistance. The value of k_{dif} ($\text{mg g}^{-1} \text{min}^{-1/2}$) can be obtained from the slope and the value of C can be obtained from y -intercept of the graph q_t vs. $t^{1/2}$.

The results obtained in the kinetics study used the Langmuir, Freundlich, Langmuir–Freundlich and Fritz–Schlunder models of adsorption to evaluate the data of the equilibrium process. These models (Eqs. (6)–(9)) are widely used to evaluate adsorption isotherms [23].

$$q_e = \frac{q_{max}K_L C_e}{1 + K_L C_e} \quad (6)$$

$$q_e = K_F C_e^{1/n} \quad (7)$$

$$q_e = \frac{q_{max}K_{LF}C_e^{1/n}}{1 + K_{LF}C_e^{1/n}} \quad (8)$$

$$q_e = \frac{K_{FS}C_e^{b_1}}{1 + aC_e^{b_2}} \quad (9)$$

where C_e is the equilibrium concentration of the adsorbate (mg L^{-1}), q_{max} (mg g^{-1}) and K_L (L mg^{-1}) are the Langmuir constants related to the maximum adsorption capacity and energy adsorption, respectively. The intensity of adsorption is $1/n$ and K_F (mg g^{-1}) (mg L^{-1}) $^{-1/n}$ is the adsorption capacity related to the Freundlich isotherm. K_{LF} (L mg^{-1}) $^{-1/n}$ is the constant of the Langmuir–Freundlich isotherm. The constants from the Fritz–Schlunder isotherm include K_{FS} (mg g^{-1}) (mg dm^{-3}) $^{-b_1}$, a (mg dm^{-3}) $^{-b_2}$ and the heterogeneity factors b_1 and b_2 .

3. Results and discussion

3.1. Characterization of the adsorbent material

3.1.1. Measurement of surface area for the adsorption/desorption of N_2 (BET)

Characterizing the orange peel using the BET method obtained a surface area of $2.14 \text{ m}^2 \text{ g}^{-1}$ with a pore volume of $4.8710^{-4} \text{ cm}^3 \text{ g}^{-1}$ a pore size of 9.24 \AA . A similar result was obtained by Liang et al. [49]. A material with this pore size is classified according to the IUPAC as a microporous material.

3.1.2. pH_{zpc} of the adsorbent

The point of zero charge, or pH_{zpc} , is a parameter indicating the pH value at which a solid particle surface has a zero charge. This parameter is important, because it can predict the charge on the adsorbent surface in relation to the pH.

Fig. 1 shows the result obtained from the tests carried out with the orange peel adsorbent in 50 mL of solution with pH ranging from 2 to 10.

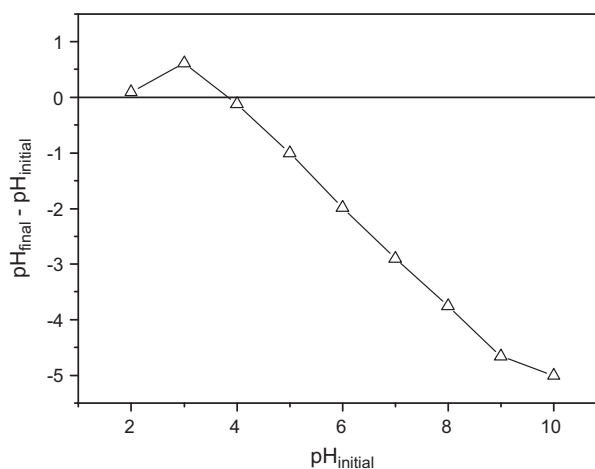


Fig. 1. pH_{zpc} of the orange peel adsorbent.

According to Fig. 1, the pH_{zpc} of the orange peel was 3.9 and indicates that below this value the solid has a positive surface charge promoting the adsorption of anions, and above this value, the surface is negatively charged, favoring adsorption of cations. The reactive gray BF-2R dye is considered an azo dye and presents various functional groups, especially negatively charged sulfonate groups. The dye interaction with the surface of the adsorbent may occur via the protonated groups of the solid interacting with the anionic groups of the dye.

3.1.3. Fourier transform infrared spectroscopy

Several chemical groups, such as carbonyl, hydroxyl, and sulfonate are considered responsible for adsorption into biomass and their importance is dependent on factors such as the number and accessibility of their sites, the chemical state and the adsorbate/adsorbent affinity. The presence of these groups was confirmed by FT-IR (Fourier transform infrared spectroscopy) analysis. Fig. 2 shows the infrared spectra of orange peel. A number of absorption peaks can be observed, indicating the complex nature of the analyzed biomass.

There is a broad band in the region of $3,472\text{ cm}^{-1}$ corresponding to the stretching vibration by hydrogen bonding in the hydroxyl molecule(OH) of alcoholic, phenolic, and carboxylic groups and stretching of the amino group N-H. These groups are associated with the cellulose and cell wall proteins of biomass.

The peak at $2,924\text{ cm}^{-1}$ corresponding to the asymmetrical stretching frequency of aliphatic CH bonds present in the cellulose and the peak at $1,740\text{ cm}^{-1}$ are both due to stretching of the carbonyl (C=O) of the

carboxylic groups (–COOH). The peak at $1,516\text{ cm}^{-1}$ corresponds to the asymmetrical stretching of the carboxylate (–COO–). The peak at $1,423\text{ cm}^{-1}$ is due to the symmetrical stretching of the carbonyl (C=O).

The bands at approximately $1,373\text{ cm}^{-1}$ correspond to the asymmetrical stretching of the sulfonic groups (–SO₃). These groups are mainly present in the sulfonic acids of polysaccharides. The peak at approximately $1,242\text{ cm}^{-1}$ corresponds to the CO stretching and deformation of the O-H of the carboxyl groups. The peak at $1,165\text{ cm}^{-1}$ is due to the symmetrical stretching of sulfonic groups (–SO₃). The peak at 833 cm^{-1} may correspond to stretching S=O, as observed by Liang et al. [49].

3.2. Adsorption experiments

3.2.1. Effect of dye solution pH

The initial pH of the solution affects the dissociation of the functional groups present on the surface of the active sites. The influence of the solution pH on the adsorption of reactive gray BF-2R dye was investigated from pH 2–10 and observed that the adsorption capacity of the orange peel was greatest at pH 2, as shown in Fig. 3.

The adsorption of the dye was higher in the most acidic solution. According to Kimura [4] the reactive dye molecules that have vinyl sulfone groups may be deprotonated in an acidic environment, resulting in a polar molecule (–SO₃–R) with a high negative charge density. This observation reinforces the result obtained in the earlier study of the pH_{zpc} of the orange peel. A similar result was also obtained by Schimmel [14], who used activated carbon for the adsorption of textile dyes.

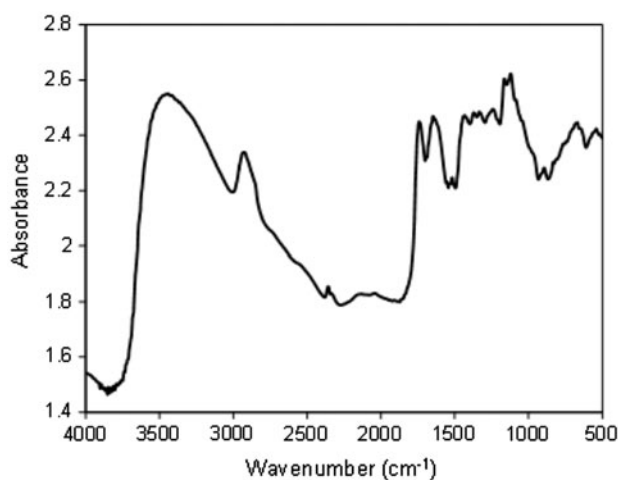


Fig. 2. Infrared spectra of orange peel.

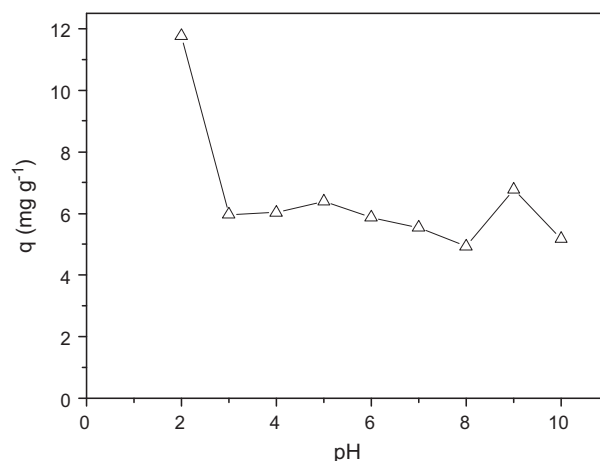


Fig. 3. An evaluation of the effect of pH on the adsorption capacity for orange peel.

3.2.2. Adsorbent concentration study

The effect of mass variation of the adsorbent in adsorption of the reactive gray BF-2R dye is shown in Fig. 4.

As seen in Fig. 4, an increase in the adsorbent concentration increases the removal of dye from 62% to 97% until removal remains constant, indicating saturation of the adsorbent. This behavior occurs because the number of active sites for interaction with the dye has increased. However, the adsorptive capacity decreases from 8.7 mg g^{-1} to 1.7 mg g^{-1} with increased adsorbent concentration due to a reduction in the adsorbate/adsorbent ratio.

The intersection between the curves of adsorption capacity and the percentage of dye removal was approximately 10 g L^{-1} . This mass/volume ratio was used as the central point of the factorial design to improve this relationship.

3.2.3. Factorial design

The influence of the mass of the adsorbent, the adsorbent particle size and stirring speed were evaluated using a 2^3 factorial design. The response in terms of adsorption capacity was used to evaluate the adsorption efficiency of the reactive gray BF-2R dye.

The calculations of the effects of factors and interactions between them showed that all parameters at levels studied were statistically significant at a 95% confidence level. This can be best illustrated through the Pareto chart in Fig. 5.

The main effects values of the mass and particle size were negative, the former more important among other main effects, namely by increasing the mass of adsorbent from 0.25 g to 0.75 g, a mean reduction in the adsorptive capacity value of 50.7% occurred.

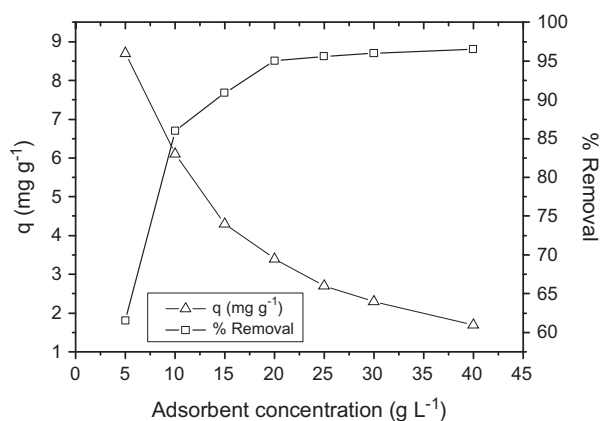


Fig. 4. The effect of varying the mass of orange peel on the adsorption of dye.

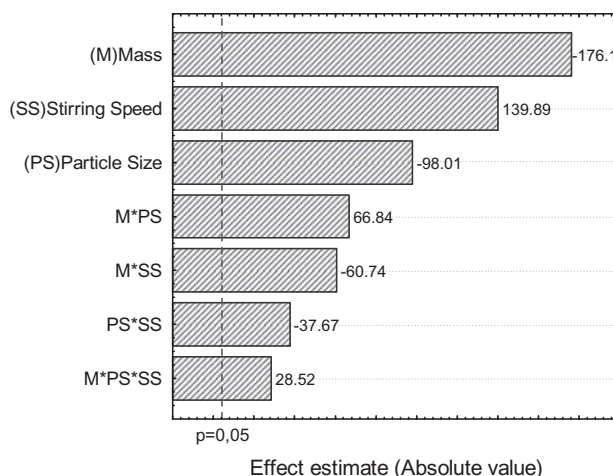


Fig. 5. Pareto chart of the calculated effects with pure error of 0.0007.

The highest adsorption capacity was obtained for 0.25 g adsorbent mass, with a particle size $<0.419 \text{ mm}$ at 300 rpm.

The response surfaces relating to the interactions of these two significant factors are shown in Fig. 6.

Fig. 6(A) shows that the highest adsorption capacity was obtained with smaller mass and particle size values. Fig. 6(B) and 6(C) show that the most adsorption capacity was obtained at higher stirring speed and smaller adsorbent mass and particle size.

Experimental data analyzed with the Statistica 6.0 program obtained an empirical model shown in Eq. (10), able to predict the adsorption capacity q of orange peel for the reactive gray BF-2R dye within the study interval, for the three variables.

$$q(\text{mg g}^{-1}) = 4.37810 - 1.52986 M - 0.85136 PS + 1.21514 SS + 0.58180 M \times PS - 0.52870 M \times SS - 0.32787 PS \times SS + 0.24873 M \times PS \times SS \quad (10)$$

Fig. 7 shows the relationship between the experimentally obtained values and those predicted by the model.

It can be observed that the data predicted by the model correlated well with the experimental data at a 95% confidence level.

3.3. Kinetics and equilibrium adsorption studies

The kinetic evolution of the removal process of the reactive gray BF-2R dye by orange peel was evaluated experimentally in tests with time varying between 0 to 360 min, as shown in Fig. 8.

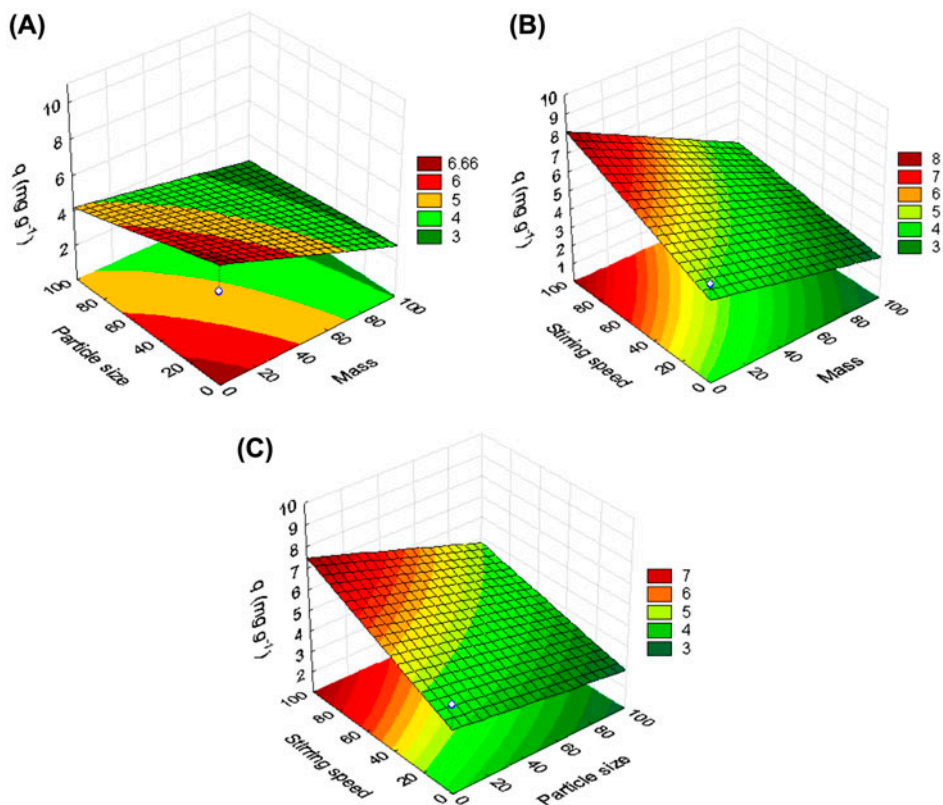


Fig. 6. Response surface for the adsorption capacity. (A) Mass vs. particle size, (B) mass vs. stirring speed, (C) particle size vs. stirring speed.

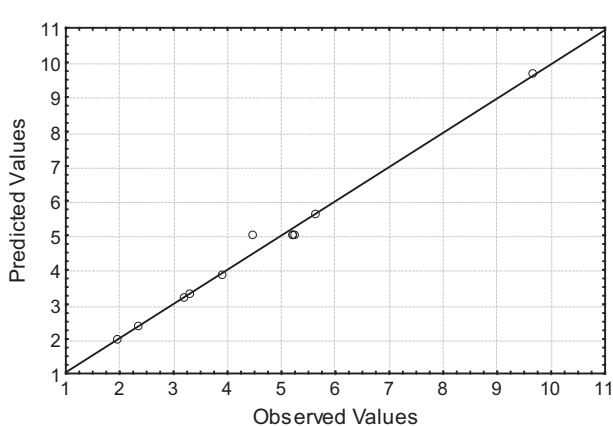


Fig. 7. Comparison between experimental values and those obtained by the model.

It was observed that the adsorption amount, q , increases with the contact time for all concentrations. Moreover, q also increases according to the initial concentration of dye in the solution.

Fig. 9 also shows the reaction proceeds rapidly in the first 10 min. Thereafter, the speed decreases, reaching saturation in 180 min. The results of the nonlinear

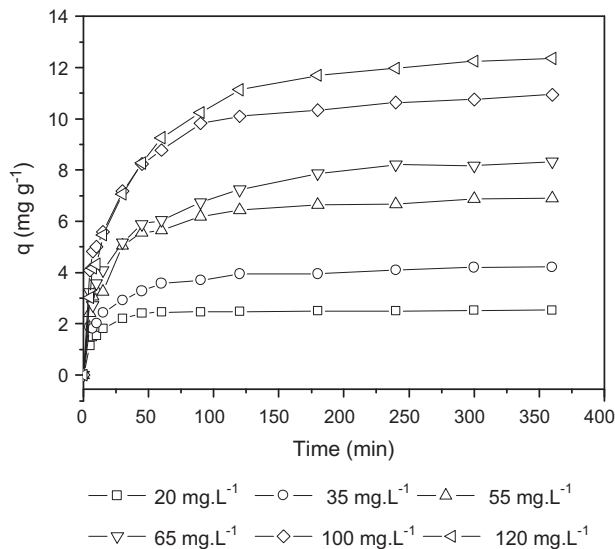


Fig. 8. Adsorption kinetics for different initial concentrations of dye.

adjustment of the pseudo-first-order and pseudo-second-order kinetic models to the experimental data are shown in Fig. 9.

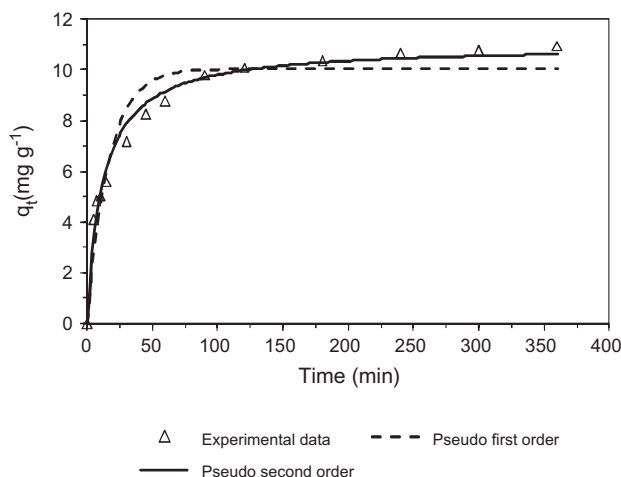


Fig. 9. Kinetic evolution of adsorption of the reactive gray BF-2R dye on orange peel.

Fig. 9 and the result obtained from the *F*-test ($F_{cal} (3.89) > F_{tab} (2.69)$), considering a confidence level of 95%, show the pseudo-second-order model was a better fit to the experimental data.

The kinetics parameters for the pseudo-first-order and pseudo-second-order models are shown in Table 1.

The kinetics data were also analyzed to determine whether the intraparticle diffusion rate is the limiting step of adsorption. In this study, the linear regression by parts method was used for data adjustment, as shown in Fig. 10.

The Weber–Morris equation did not satisfy a linear relation with the experimental data, which was multi-linear. This result, as Uma et al. [50] demonstrated, indicates that the adsorption process is not just controlled by an intraparticle diffusion step. This means that two or more steps control the process.

The first portion of the curve of greatest slope corresponds to the external surface adsorption phase; the second is the gradual adsorption phase, in which the intraparticle diffusion is controlling the process; the third is the final phase of equilibrium, in which intraparticle diffusion begins to attenuate due to the

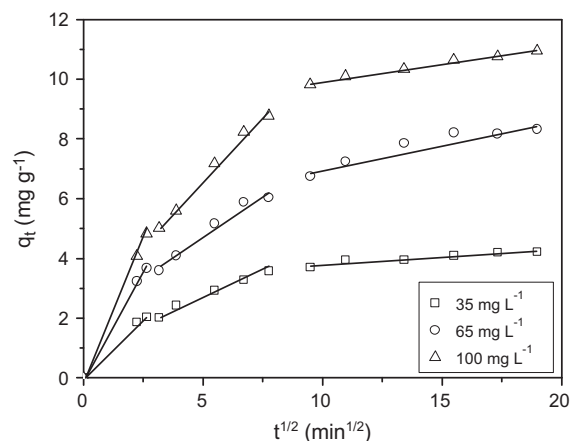


Fig. 10. Intraparticle diffusion Weber–Morris model.

Table 2
Intraparticle diffusion Weber–Morris model constants

Step	35 mg L ⁻¹			65 mg L ⁻¹			100 mg L ⁻¹		
	k_{dif}	C	R ²	k_{dif}	C	R ²	k_{dif}	C	R ²
1	0.79	0.01	0.99	1.41	0.01	0.99	1.82	0.0003	1.00
2	0.33	1.07	0.99	0.56	1.94	0.97	0.85	2.38	0.99
3	0.05	3.29	0.90	0.16	5.45	0.89	0.12	8.78	0.99

low concentration of the solute in solution. Comparing the three constants (k_{dif1} , k_{dif2} , k_{dif3}), we can see that $k_{dif1} > k_{dif2} > k_{dif3}$ [51], as seen in Table 2.

The values of C give an indication of the boundary layer thickness, namely the higher the value of C, the greater the effect of the boundary layer. When the values of C are nonzero, this indicates that the line of the graph q_t vs. $t^{1/2}$ (Fig. 10) does not pass through the origin. Therefore, the mechanism of intraparticle diffusion is not the determining step in the process of mass transfer and other mechanisms must operate simultaneously to control the adsorption process [52].

In the study of equilibrium adsorption, the isotherms of Langmuir, Freundlich, Langmuir–Freundlich

Table 1
Kinetics parameters for the pseudo-first-order and pseudo-second-order models

Pseudo-first-order				
k_1 (min ⁻¹)	q_e calc. (mg g ⁻¹)	q_e exp. (mg g ⁻¹)	R ²	S_R^2 (mg ² g ⁻²)
0.06 ± 0.01	10.0 ± 0.3	10.6 ± 0.4	0.92	0.21
Pseudo-second-order				
k_2 (g mg ⁻¹ min ⁻¹)	q_e calc. (mg g ⁻¹)	q_e exp. (mg g ⁻¹)	R ²	S_R^2 (mg ² g ⁻²)
0.08 ± 9 × 10 ⁻⁴	10.9 ± 0.2	10.6 ± 0.4	0.98	0.83

Table 3
Equilibrium parameters

q_{\max} (mg g ⁻¹)	K_L (L mg ⁻¹)	R^2	S_R^2 (mg ² g ⁻²)	K_{LF} (mg g ⁻¹) (mg dm ⁻³) ^{-b₁}	a (mg dm ⁻³) ^{-b₂}	b_1	b_2	R^2	S_R^2 (mg ² g ⁻²)
Langmuir model									
12.0 ± 0.5	0.45 ± 0.08	0.97	0.36	Fritz–Schlunder model	0.4 ± 0.2	0.8 ± 0.1	0.83 ± 0.04	0.99	0.09
Freundlich model									
K_F (mg g ⁻¹) (mg L ⁻¹) ^{-1/n}	n	R^2	S_R^2 (mg ² g ⁻²)	Langmuir–Freundlich model	K_{LF} (L mg ⁻¹) ^{-1/n}	n	R^2	S_R^2 (mg ² g ⁻²)	
4.4 ± 0.4	3.5 ± 0.4	0.95	0.56		0.39 ± 0.06	1.5 ± 0.2	0.99	0.14	

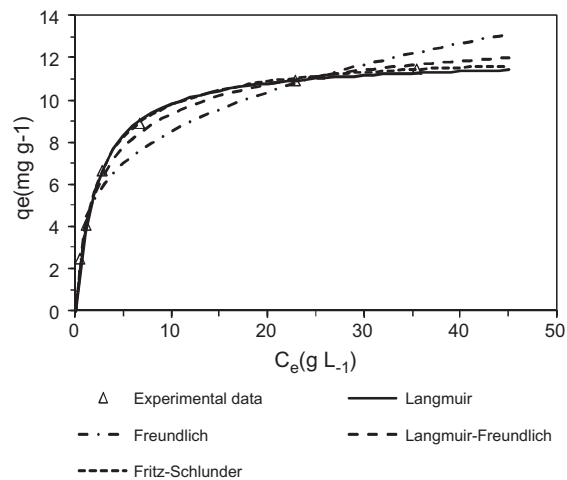


Fig. 11. Adjustment of the nonlinear models of adsorption.

and Fritz–Schlunder were used. Fig. 11 shows the settings of these nonlinear models to experimental data.

In Fig. 11, the Langmuir and Fritz–Schlunder models were evaluated using *F-test*. The result from the *F-test* ($F_{cal} (3.83) < F_{tab} (19.25)$), at a confidence level of 95%, showed that although the model of Fritz–Schlunder is applied to liquid–solid systems, the Langmuir model showed a very similar behavior with no significant differences between the two models.

Table 3 presents the values of the parameters obtained for the models of Langmuir, Freundlich, Langmuir–Freundlich and Fritz–Schlunder.

4. Conclusion

The characterization of orange peel revealed that the material is microporous and that it has a pH_{zpc} of 3.9 and contains carboxylic and sulfonic groups that are responsible for the adsorption of biomass.

The study of adsorption of the reactive gray BF-2R dye by orange peel showed that the process is highly affected by pH, with the best capacity at pH 2.0. This result is justified by the pH_{zpc} of the material and the presence of sulfonate groups in the dyes, which interact stronger with the solid when the surface is protonated.

In the factorial design, the highest value of q was achieved with 0.25 g of adsorbent mass and particle size <0.419 mm and 300 rpm, and this condition was used in the subsequent kinetics and equilibrium adsorption studies.

The kinetics study showed that reaction proceeds rapidly for the first 10 min and thereafter the speed decreases, reaching saturation in 180 min. The pseudo-second-order model showed a better fit to the experimental data with parameters of k_2 equal to $0.08 \pm 9 \times 10^{-4} \text{ g mg}^{-1} \text{ min}^{-1}$ and $q_{e,\text{calc.}}$ of $10.9 \pm 0.2 \text{ mg g}^{-1}$. The Weber–Morris model indicated that two or more mechanisms control the process.

In the study of equilibrium showed that although the Fritz–Schlunder model is generally applied to liquid–solid systems, the Langmuir model showed similar behavior with no significant differences between the two models.

The results showed that orange peel has the potential to remove reactive gray BF-2R dye from aqueous solutions and can be employed as an effective biosorbent.

Acknowledgements

Conselho Nacional de Desenvolvimento Científico e Tecnológico (CNPq) for financial support and Texpal for providing the reactive gray BF-2R dye.

Symbols

Q	$[\text{mg g}^{-1}]$	— adsorption capacity
C_0	$[\text{mg L}^{-1}]$	— initial concentration
C_f	$[\text{mg L}^{-1}]$	— final concentration
V	$[\text{L}]$	— volume of solution
M	$[\text{g}]$	— adsorbent mass
PS	$[\text{mm}]$	— adsorbent particle size
SS	$[\text{rpm}]$	— stirring speed
σ_i	—	— relative standard deviation
R^2	—	— regression coefficient
$S_R^2(A)$	$[\text{mg}^2 \text{g}^{-2}]$	— deviation of model A
$S_R^2(B)$	$[\text{mg}^2 \text{g}^{-2}]$	— deviation of model B
q_e	$[\text{mg g}^{-1}]$	— adsorption capacity at equilibrium
q_t	$[\text{mg g}^{-1}]$	— adsorption capacity at time t
t	$[\text{min}]$	— time
k_1	$[\text{min}^{-1}]$	— adsorption constant of the pseudo-first-order equation
k_2	$[\text{g mg}^{-1} \text{ min}^{-1}]$	— adsorption constant of the pseudo-second-order equation
k_{dif}	$[\text{mg g}^{-1} \text{ min}^{-1/2}]$	— intra particle diffusion coefficient
C	$[\text{mg g}^{-1}]$	— constant related to diffusion resistance
C_e	$[\text{mg L}^{-1}]$	— equilibrium concentration
q_{max}	$[\text{mg g}^{-1}]$	— maximum adsorption capacity
K_L	$[\text{L mg}^{-1}]$	— Langmuir constant
$1/n$	—	— intensity of adsorption
K_F	$[\text{mg g}^{-1}]$ $[\text{mg L}^{-1}]^{-1/n}$	— adsorption capacity related to the Freundlich isotherm

K_{LF}	$[\text{L mg}^{-1}]^{-1/n}$	— Langmuir–Freundlich Constant
K_{FS}	$[\text{mg g}^{-1}]$ $[\text{mg dm}^{-3}]^{-b_1}$	— Fritz–Schlunder Constant
a	$[\text{mg dm}^{-3}]^{-b_2}$	— Fritz–Schlunder Constant
b_1	—	— factor of heterogeneity
b_2	—	— factor of heterogeneity

References

- [1] A. Saeed, M. Sharif, M. Iqbal, Application potential of grapefruit peel as dye sorbent: Kinetics, equilibrium and mechanism of crystal violet adsorption, *J. Hazard. Mater.* 179 (2010) 564–572.
- [2] A. Mittal, J. Mittal, A. Malviya, D. Kaur, V.K. Gupta, Decoloration treatment of a hazardous triarylmethane dye, Light Green SF (Yellowish) by waste material adsorbents, *J. Colloid Interface Sci.* 342 (2010) 518–527.
- [3] A. Mittal, J. Mittal, A. Malviya, D. Kaur, V.K. Gupta, Adsorption of hazardous dye crystal violet from wastewater by waste materials, *J. Colloid Interface Sci.* 343 (2010) 463–473.
- [4] R. Kumar, R. Ahmad, Biosorption of hazardous crystal violet dye from aqueous solution onto treated ginger waste (TGW), *Desalination* 265 (2011) 112–118.
- [5] B.H. Hameed, A.A. Ahmad, Batch adsorption of methylene blue from aqueous solution by garlic peel, an agricultural waste biomass, *J. Hazard. Mater.* 164 (2009) 870–875.
- [6] A. Mittal, D. Kaur, J. Mittal, Applicability of waste materials-bottom ash and deoiled soya-as adsorbents for the removal and recovery of a hazardous dye, brilliant green, *J. Colloid Interface Sci.* 326 (2008) 8–17.
- [7] X. Li, W. Xiao, G. He, W. Zheng, N. Yu, M. Tan, Pore size and surface area control of MgO nanostructures using a surfactant-templated hydrothermal process: High adsorption capability to azo dyes, *Colloids Surf., A* 408 (2012) 79–86.
- [8] I. Kimura, A. Gonçalves Jr., J. Solberg, Effects of pH and contact time on adsorption of reactive dyes on chitosan microspheres, *Polímeros*. 9 (1999) 51–57.
- [9] E. Forgacs, T. Cserhádi, G. Oros, Removal of synthetic dyes from wastewaters: a review, *Environ. Int.* 30 (2004) 953–971.
- [10] H. Zollinger, *Color chemistry*, third ed., Verlag Helvetica ChimicaActa, Switzerland, 2003.
- [11] M.R. Zamanloo, A.N. Shamkhali, M. Alizadeh, Y. Mansoori, G. Imanzadeh, A novel barbituric acid-based azo dye and its derived polyamides: Synthesis, spectroscopic investigation and computational calculations, *Dyes and Pigments* 95 (2012) 587–599.
- [12] H.M. Pinheiro, E. Touraud, O. Thomas, Aromatic amines from azo dye reduction: status review with emphasis on direct UV spectrophotometric detection in textile industry wastewaters, *Dyes and Pigments* 61 (2004) 121–139.
- [13] F. Atmani, A. Bensmaili, N.Y. Mezenner, Synthetic textile effluent removal by skin almonds waste, *Environ. Sci. Technol.* 2 (2009) 53–169.
- [14] B.H. Tan, T.T. Teng, A.K.M. Omar, Removal of dyes and industrial dye wastes by magnesium chloride, *Water Res.* 34 (2000) 597–601.
- [15] S.A. Parsons, B. Jeffersons, *Introduction to Potable Water Treatment Process*, first ed., Blackwell Publishing, Oxford, 2006.
- [16] P. Mavros, A.C. Danilidou, N.K. Lazaridis, L. Stergiou, Color removal from aqueous solutions. Part I. Flotation, *Environ. Technol.* 15 (1994) 601–616.

(Continued)

- [17] A.I. Zouboulis, N.K. Lazaridis, A. Grohmann, Toxic metals removal from waste waters by upflow filtration with floating filter medium. I. The case of zinc, *Sep. Sci. Technol.* 37 (2002) 403–416.
- [18] B. Bolto, D. Dixon, R. Eldridge, S. King, K. Linge, Removal of natural organic matter by ion exchange, *Water Res.* 36 (2002) 5057–5065.
- [19] T.M. Lapara, A. Konopka, C.H. Nakatsu, J.E. Alleman, Thermophilic aerobic wastewater treatment in continuous-flow bioreactors, *J. Environ. Eng.* 126 (2000) 739–744.
- [20] J. Bell, J.J. Plumb, C. A. Buckley, D.C. Stuckey, Treatment and decolorization of dyes in an anaerobic baffled reactor, *J. Environ. Eng.* 126 (2000) 1026–1032.
- [21] A. Pala, E. Tokat, Color removal from cotton textile industry wastewater in an activated sludge system with various additives, *Water Res.* 36 (2002) 2920–2925.
- [22] C.F. Schutte, The rejection of specific organic compounds by reverse osmosis process, *Desalination* 158 (2003) 285–295.
- [23] A.B. Karim, B. Mounir, M. Hachkar, M. Bakasse, A. Yaacoubi, Removal of Basic Red 46 dye from aqueous solution by adsorption onto moroccan clay, *J. Hazard. Mater.* 168 (2009) 304–309.
- [24] M.L. Soto, A. Moure, H. Domínguez, J.C. Parajó, Recovery, concentration and purification of phenolic compounds by adsorption: a review, *J. Food Eng.* 105 (2011) 1–27.
- [25] A. Mittal, V. Thakur, V. Gajbe, Evaluation of adsorption characteristics of an anionic azo dye Brilliant Yellow onto hen feathers in aqueous solutions, *Environ. Sci. Pollut. Res.* 19 (2012) 2438–2447.
- [26] A. Mittal, V. Thakur, V. Gajbe, Adsorptive removal of toxic azo dye Amido Black 10B by hen feather, *Environ. Sci. Pollut. Res.* 20 (2013) 260–269.
- [27] A. Mittal, J. Mittal, L. Kurup, Utilization of Hen Feathers for the Adsorption of Indigo Carmine from Simulated Effluents, *J. Environ. Protect. Sci.* 1 (2007) 92–100.
- [28] V.K. Gupta, A. Mittal, D. Jhare, J. Mittal, Batch and bulk removal of hazardous colouring agent Rose Bengal by adsorption techniques using bottom ash as adsorbent, *RSC Adv.* 2 (2012) 8381–8389.
- [29] C.Y. Tan, M. Li, Y.M. Lin, X.Q. Lu, Z.L. Chen, Biosorption of Basic Orange from aqueous solution onto dried *A. filiculoides* biomass: Equilibrium, kinetic and FTIR studies, *Desalination* 266 (2011) 56–62.
- [30] A. Mittal, V. Gajbe, J. Mittal, Removal and recovery of hazardous triphenylmethane dye, Methyl Violet through adsorption over granulated waste materials, *J. Hazard. Mater.* 150 (2008) 364–375.
- [31] A. Mittal, R. Jain, J. Mittal, S. Varshney, S. Sikarwar, Removal of Yellow ME 7 GL from industrial effluent using electrochemical and adsorption techniques, *Int. J. Environ. Pollut.* 43 (2010) 308–323.
- [32] V.K. Gupta, Suhas, Application of low-cost adsorbents for dye removal – a review, *J. Environ. Manage.* 90 (2009) 2313–2342.
- [33] D. Sud, G. Mahajan, M.P. Kaur, Agricultural waste material as potential adsorbents for sequestering heavy metal from aqueous solutions – a review, *Bioresour. Technol.* 99 (2008) 6017–6027.
- [34] M. Achak, A. Hafidi, N. Ouazzani, S. Sayadi, L. Mandi, Low cost biosorbent “banana peel” for the removal of phenolic compounds from olive mill wastewater: Kinetic and equilibrium studies, *J. Hazard. Mater.* 166 (2009) 117–125.
- [35] G. Crini, Non-conventional low-cost adsorbents for dye removal: a review, *Bioresour. Technol.* 97 (2006) 1061–1085.
- [36] A. Mittal, D. Jhare, J. Mittal, Adsorption of hazardous dye Eosin Yellow from aqueous solution onto waste material De-oiled Soya: Isotherm, kinetics and bulk removal, *J. Mol. Liq.* 179 (2013) 133–140.
- [37] A. Mittal, J. Mittal, L. Kurup, A.K. Singh, Process development for the removal and recovery of hazardous dye erythro-sine from wastewater by waste materials – bottom ash and de-oiled soya as adsorbents, *J. Hazard. Mater.* 138 (2006) 95–105.
- [38] A. Mittal, D. Kaur, A. Malviya, J. Mittal, V.K. Gupta, Adsorption studies on the removal of coloring agent phenol red from wastewater using waste materials as adsorbents, *J. Colloid Interface Sci.* 337 (2009) 345–354.
- [39] A. Mittal, D. Kaur, J. Mittal, Batch and bulk removal of a tri-arylmethane dye, Fast Green FCF, from wastewater by adsorption over waste materials, *J. Hazard. Mater.* 163 (2009) 568–577.
- [40] O.R.S. Rocha, G.E. Nascimento, N.F. Campos, V.L. Silva, M.M.M.B. Duarte, Evaluation of adsorption process using green coconut mesocarp for removal of reactive gray BF-2R dye, *Quim. Nova* 35 (2012) 1369–1374.
- [41] C.C.A. Leal, O.R.S. Rocha, M.M.M.B. Duarte, R.F. Dantas, M.A. MottaSobrinho, N.M. LimaFilho, V.L. Silva, Evaluation of the adsorption process of remazol black B dye in liquid effluents by green coconut mesocarp, *Afinidad LXVI* 546 (2010) 136–142.
- [42] S. Jain, R. V. Jayaram, Removal of basic dyes from aqueous solution by low-cost adsorbent: Wood apple shell (*Feroniaacidissima*), *Desalination* 250 (2010) 921–927.
- [43] F.A. Pavan, Y. Gushikem, A.S. Mazzocato, S.L.P. Dias, E.C. Lima, Statistical design of experiments as tool for optimizing the batch conditions to methylene blue adsorption on yellow passion fruit and mandarin peels, *Dyes and Pigments* 72 (2007) 256–266.
- [44] R.O. Cristóvão, A.P.M. Tavares, A.I. Brígida, J.M. Loureiro, R.A.R. Boaventura, E.A. Macedo, M.A.Z. Coelho, Immobilization of commercial laccase onto green coconut fiber by adsorption and its application for reactive textile dyes degradation, *J. Mol. Catal. B: Enzym.* 72 (2011) 6–12.
- [45] D. Schimmel, Dissertation, Universidade Estadual do Oeste do Paraná, Toledo-PR, Brasil, 2008.
- [46] B. Barros Neto, I.S. Scarminio, R.E. Bruns, *Como Fazer Experimentos: Pesquisa e desenvolvimento na ciência e na indústria*, 3^a ed., Unicamp, Campinas, 2007.
- [47] D.C. Montgomery, *Design and analysis of experiments*, fifth ed., John Wiley & Sons, New York, NY, 2001.
- [48] V. Vadivelan, K.V. Kumar, Equilibrium, kinetics, mechanism, and process design for the sorption of methylene blue onto rice husk, *J. Colloid Interface Sci.* 286 (2005) 90–100.
- [49] S. Liang, X. Guo, N. Feng, Q. Tian, Isotherms, kinetics and thermodynamic studies of adsorption of Cu²⁺ from aqueous solutions by Mg²⁺/K⁺ type orange peel adsorbents, *J. Hazard. Mater.* 174 (2010) 756–762.
- [50] R.L. Uma, V.C. Srivastava, I.D. Mall, D.H. Lataye, Rice husk ash as an effective adsorbent: Evaluation of adsorptive characteristics for Indigo Carmine dye, *J. Environ. Manage.* 90 (2009) 710–720.
- [51] O. Gulnaz, S. Saygideger, E. Kusvuran, Study of Cu(II) biosorption by dried activated sludge: effect of physico-chemical environment and kinetics study, *J. Hazard. Mater.* 120 (2005) 193–200.
- [52] N. Dizge, C. Aydinler, E. Demirbas, M. Kobya, S. Kara, Adsorption of reactive dyes from aqueous solutions by fly ash: kinetic and equilibrium studies, *J. Hazard. Mater.* 150 (2008) 737–747.